

## RESEARCH ARTICLE

10.1002/2017JA023914

## Key Points:

- The lightning-induced perturbation in DTEC data is periodic, and computed periodicities are found to be ranging from few tens of minutes to hundreds of minutes
- Possible plasma bubble signatures in GPS-STEC data and their association with strong amplitude scintillations have been observed
- TEC perturbations are attributed to the combined effect of lightning-induced electric field and GWs in the convective region of thunderstorm

## Correspondence to:

S. Kumar,  
sanjay.skitvns@gmail.com

## Citation:

Kumar, S., W. Chen, M. Chen, Z. Liu, and R. P. Singh (2017), Thunderstorm-/lightning-induced ionospheric perturbation: An observation from equatorial and low-latitude stations around Hong Kong, *J. Geophys. Res. Space Physics*, 122, 9032–9044, doi:10.1002/2017JA023914.

Received 20 JAN 2017

Accepted 9 AUG 2017

Accepted article online 15 AUG 2017

Published online 31 AUG 2017

Corrected 12 SEP 2017

This article was corrected on 12 SEP 2017. See the end of the full text for details.

## Thunderstorm-/lightning-induced ionospheric perturbation: An observation from equatorial and low-latitude stations around Hong Kong

Sanjay Kumar<sup>1,2</sup> , Wu Chen<sup>1</sup> , Mingli Chen<sup>3</sup>, Zhizhao Liu<sup>1</sup> , and R. P. Singh<sup>2</sup>

<sup>1</sup>The Department of Land Surveying and Geo-Informatics, The Hong Kong Polytechnic University, Hong Kong, <sup>2</sup>Department of Physics, Banaras Hindu University, Varanasi, India, <sup>3</sup>Department of Building Services Engineering, Hong Kong Polytechnic University, Hong Kong

**Abstract** Total electron content (TEC) computed from the network of Global Positioning System over Hong Kong area known as Hong Kong Sat-Ref-network has been used to study perturbation in the ionosphere from thunder storm activity. Data for geomagnetic quiet day ( $K_p < 4$ , on 1 April 2014) have been analyzed. The lightning activity was measured from Total Lightning sensor LS8000 over/around the Hong Kong region. Deviation in vertical TEC (DTEC) and the rate of change of TEC index (ROTI) have been derived and compared for lightning day of 1 April 2014 and nonlightning day of 7 April 2014. An analysis showed reduction in TEC during evening hour (up to 1245 UT), whereas an enhancement during nighttime hour on the lightning day is observed. The variations in DTEC during nonlightning day are found to be insignificant in comparison to that during the lightning day. The ionospheric perturbation in TEC has been noticed up to a distance around  $\sim 500$  km and more from the lightning center. ROTI is found to vary from 3 to 60 total electron content unit (TECU)/min ( $1 \text{ TECU} = 10^{16} \text{ el m}^{-2}$ ) on the day of thunderstorm activity, whereas ROTI is insignificant on nonlightning days. Signature of density bubbles in slant TEC data and periodicities (10–100 min) in DTEC data are observed. For the same pseudorandom numbers (1, 10, 13, 23, and 28) strong amplitude scintillations are also observed at a close by station. Amplitude scintillations are proposed to be caused by plasma bubbles. The results are tentatively explained by thunderstorm-induced electric fields and gravity waves.

### 1. Introduction

Thunderstorms are electric generators, which drive upward currents in the global electric circuit [Williams, 2009; Singh et al., 2012]. In the global circuit the total time-averaged current from cloud-to-ground lightning and intracloud lightning may lie between 50 and 400 A [Mareev et al., 2008], whereas peak current may vary up to few tens of kiloampere. The upward current is associated with electric field which may cause  $E \times B$  plasma drift leading to redistribution of plasma in the ionosphere and hence perturbation in electron density [Vellinov et al., 1992; Davis and Johnson, 2005; Davis and Lo, 2008; Lay et al., 2013]. Shao et al. [2012] reported that electric activity associated with even a small thunderstorm affects the *D* region by heating electrons and subsequently reducing the electron density. Kuo and Lee [2015] simulated a tripole-charge structured thunderstorm model, computed upward flowing current into the ionosphere, and its effect on electron density distribution. They showed that a source current of 8.3 A in the equatorial region may cause a change of 1–10% in total electron content.

Thunderstorms are also associated with gravity wave generation. Statistical studies show that gravity waves are prevalent above smaller, single-celled as well as mesoscale convective systems [Lay et al., 2015]. Gravity waves are generated from overshooting cloud tops of thunderstorm [Vadas and Fritts, 2004; Lay et al., 2015], may propagate vertically upward, and transfer energy from the sight of lightning into the ionosphere. Thunderstorm-originated perturbation in plasma distribution of the ionosphere is recently reported by many workers [Vadas and Fritts, 2004; Davis and Johnson, 2005; Johnson and Davis, 2006; Davis and Lo, 2008; Immel et al., 2009; Kumar et al., 2009a, 2009b; Lay et al., 2013, 2015]. Davis and Johnson [2005] reported correlation between the strength of sporadic *E* layer and lightning activity and suggested that these perturbations could be explained either by vertically upward propagating gravity waves generated from thunderstorm site or by vertical electric discharges or by a combination of these two mechanisms. Thunderstorm-associated gravity waves longer than 5 min have been observed in the *F* region [Lay et al., 2013; Vadas and Liu, 2013] as well as in

**Table 1.** List of GPS Stations Under Hong Kong CORS Network With Their Latitude and Longitude

Sl. No.	Station Code	Latitude	Longitude
1	COAL	22°, 07'N	113°, 33'E
2	DSMG	22°, 09'N	113°, 34'E
3	FOMO	22°, 11'N	113°, 32'E
4	HKKS	22°, 22'N	114°, 18'E
5	HKKT	22°, 26'N	114°, 03'E
6	HKLM	22°, 13'N	114°, 07'E
7	HKLT	22°, 25'N	113°, 59'E
8	HKMW	22°, 15'N	114°, 00'E
9	HKNP	22°, 14'N	113°, 53'E
10	HKOH	22°, 14'N	114°, 13'E
11	HKPC	22°, 17'N	114°, 02'E
12	HKSC	22°, 19'N	114°, 08'E
13	HKSL	22°, 22'N	113°, 55'E
14	HKSS	22°, 25'N	114°, 16'E
15	HKST	22°, 23'N	114°, 18'E
16	HKT	22°, 32'N	114°, 13'E
17	HKWS	22°, 26'N	114°, 20'E
18	T430	22°, 29'N	114°, 08'E

tions associated with thunderstorm activities are from midlatitude regions. In this paper an effort has been made to show large influence of thunderstorm activities on ionospheric perturbation, irregularities, and scintillation activities over near equatorial and low-latitude regions around the Hong Kong (geomagnetic latitude 12.30°–12.71°N, longitude 113.54°–114.33°E) where ionospheric variability is more dynamic and complex as compared to midlatitudes. The ionospheric TEC data derived from GPS SatRef network operating over the Hong Kong have been analyzed to study the ionospheric perturbation and irregularities caused by thunderstorm/lightning activity. The data and method of analysis are briefly described in section 2. Results and discussions are presented in sections 3 and 4, respectively. Finally, section 5 summarizes the results.

## 2. Data and Method of Analysis

The Total Lightning Sensor LS8000 installed over the Hong Kong region provides location and magnitude of lightning activity. The LS8000 is one of the two principal sensor configurations offered in the Vaisala Thunderstorm Information System ([www.vaisala.com](http://www.vaisala.com)). This sensor configuration integrates the two most effective lightning detection technologies: (i) very high frequency (VHF) interferometry and (ii) low-frequency combined magnetic direction finding and time-of-arrival measurements. VHF interferometry technology provides extremely high performance in detection of cloud lightning. The LS8000 provides unique VHF total lightning mapping of the full spatial extent and yields detailed data set of thunderstorm activity and cloud lightning information with calibrated lightning parameters.

The GPS observation data in RINEX format has been taken from the Hong Kong SatRef network as well as the International Global Navigation Satellite Systems (GNSS) Service (IGS) network. The details of all the GPS stations with their latitude and longitude are listed in Table 1. The estimated slant total electron content (STEC) is converted to vertical TEC (VTEC) using a mapping function [Kumar and Singh, 2009; Kumar et al., 2015]. In this study, the VTEC data measured by the suitable pseudorandom number (PRN) passing over the region are selected. In order to assess the effect of lightning, the TEC data for nonlightning day are estimated using the best polynomial fitting technique [Lay et al., 2013, 2015]. For a chosen PRN, the difference between lightning day VTEC data and best fitted polynomial on lightning day VTEC yields the perturbation in TEC (DTEC). In this process gross effect is removed and perturbation corresponding to phase with an accuracy of 0.01–0.1 total electron content unit (TECU; 1 TECU =  $10^{16}$  el m $^{-2}$ ) is usually achieved [Burrell et al., 2009; Lay et al., 2013, 2015]. Therefore, any perturbation in TEC >0.1 TECU has been considered as caused by lightning activity because we have considered quiet time condition (with  $K_p$  index < 4 and  $-30 < Dst$  index < 0) for both lightning and nonlightning day data. In the polynomial fitting lower frequency noises are filtered out.

the *D* region [Yue et al., 2009, 2013; Chou et al., 2016]. Lay et al. [2015] based on case studies as well as statistical studies showed that ionospheric gravity wave activities in the midlatitude U.S. Great Plains are closely associated with thunderstorm activities. They further showed that for the days of the statistical study the daily TEC decreases between 0300 and 0600 UTC to its nighttime value. This time window also correlated with gravity wave damping. The damping may have been associated with less plasma at lower (<350 km) altitudes [Ding et al., 2003].

Most of the reported studies pertaining to ionospheric perturba-

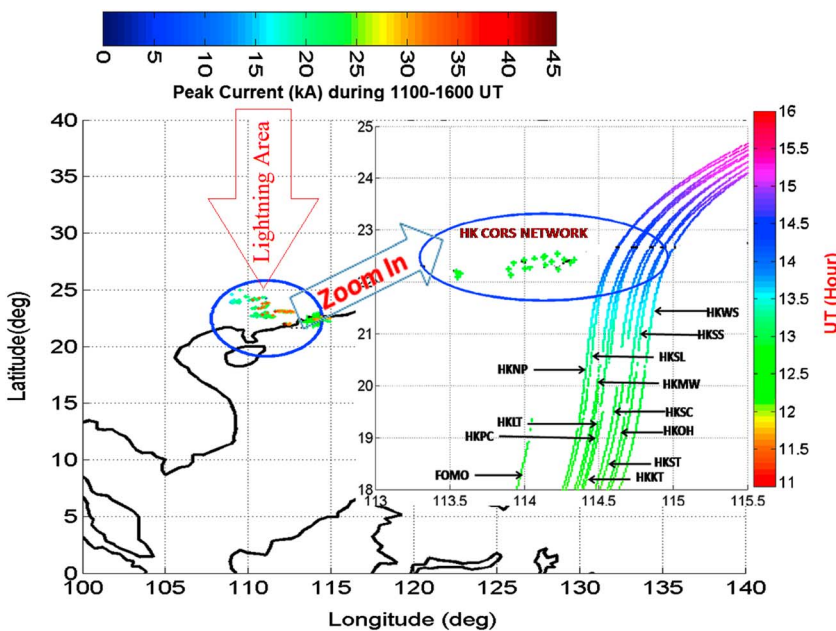


**Figure 1.** Spatial distribution of the lightning induced peak current on 1 April 2014 during 1100–1600 UT. The peak current (kA) is shown by color bar at top of figure. Each GPS station is of HK CORS network and is marked by plus signs with green color, and its zoom in form are presented on right side. The zoom in presentation of all stations and path of PRN 01 observed from all the other stations are shown on right side. The passage time (UT hour) of PRN 01 is shown by color bar on the right side of figure. Each trajectory represents the latitude, longitude of IPP (ionospheric pierce point) computed for PRN 01 observed from respective GPS station of HK CORS network.

The rate of change of TEC index (ROTI) is the standard deviation of rate of change of TEC (ROT) and is normally used to observe the ionospheric perturbation or irregularities [Pi *et al.*, 1997]. ROTI is computed from ROT data over 5 min interval having sampling of 0.5 min from the following equation:

$$\text{ROTI} = \sqrt{\langle \text{ROT}^2 \rangle - \langle \text{ROT} \rangle^2} \quad (1)$$

where ROT at epoch time  $t_k$  is given by

$$\text{ROT}(t_k) = \frac{\text{TEC}(t_k) - \text{TEC}(t_{k-1})}{t_k - t_{k-1}} \quad (2)$$

Generally, ROT is expressed in TECU/min where  $1 \text{ TECU} = 10^{16} \text{ el/m}^2$ .

The presence of plasma bubble can be seen as a sudden dip in the slant total electron content (STEC) which is followed by a recovery when the satellite-to-receiver raypath no longer passes through the bubble. Thus, a plasma bubble can be sensed in GPS-STEC data using the method proposed by Portillo *et al.* [2008]. In this method a best polynomial fit to GPS-STEC for a chosen PRN is applied with a suitable window size. The value of DSTEC is obtained by subtracting the best polynomial fitted to STEC curve from the original STEC curve. The difference between the maximum and minimum values is called as depth of the plasma bubble, which can be used as an indicator for the occurrence of bubble. The STEC depletions observed from a satellite with magnitude greater than 5 TECU and apparent duration between 10 min and 180 min are considered as a plasma bubble [Portillo *et al.*, 2008; Kumar *et al.*, 2016].

### 3. Results and Discussion

#### 3.1. Ionospheric Perturbation in TEC

The lightning data observed from the local network are used to project thunderstorm activity in a regional map of Hong Kong. Figure 1 shows the spatial distribution of selected stations and associated path of IPP

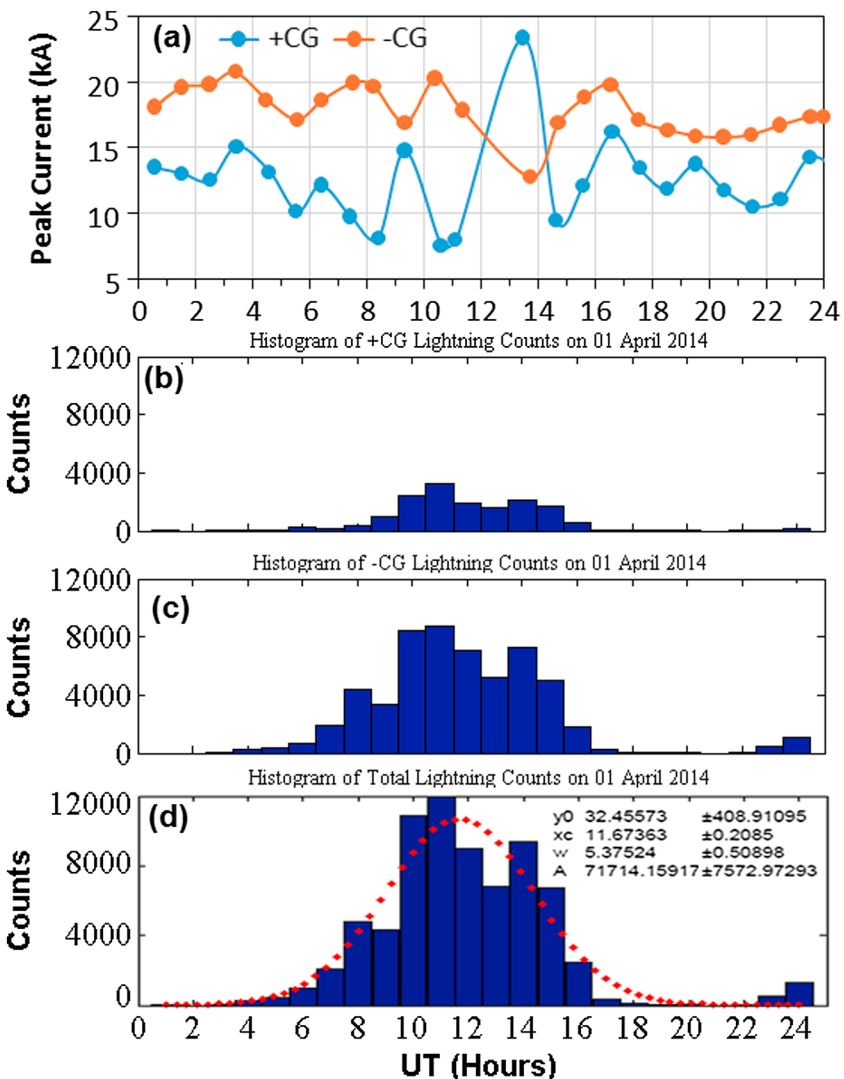


**Figure 2.** (a–d) Time series of lightning peak current 1 April 2014. The positive peak current at around 1300 UT indicates the highest lightning activity. Histograms of lightning counts (+CG, –CG, and total) during 1 h interval are also shown in bottom graphs.

along with peak current during 1100–1600 UT ( $LT = UT + 8$ ) on 1 April 2014. The observed peak current (indicated by color bar on the top of Figure 1) lies between 15 and 45 kA. Each GPS station is marked by plus sign with green color whose zoom in form is given on the right side of the figure. The path of IPPs for PRN 01 as a function of UTC observed from each GPS station of Hong Kong CORS network on 1 April 2014 is also shown. The color bar on the right side represents the passage time in UTC of PRNs. GPS stations with coordinates are also mentioned in Table 1 for precision. Figure 2 depicts the time series of hourly averaged lightning peak current associated with positive cloud-to-ground (+CG) and negative CG (–CG) lightning discharges on 1 April 2014. In addition, histogram of lightning counts (+CG, –CG, and total) over 1 h duration is also shown in the bottom graphs of Figures 2b–2d. There are substantial lightning activities during 1000–1500 UT. During this period an intense cloud movement is reported by the Hong Kong observatory. The cloud top temperature remained around  $-30^{\circ}\text{C}$  as observed from Atmospheric Infrared Sounder satellite (website: <https://giovanni.sci.gsfc.nasa.gov>). The clouds seem to be intense convective system at an altitude of about 8 km. The system seems to be capable of generating gravity waves. The GPS TEC data for PRN 01 passing over the region are available for a period between 1100 UT and 1600 UT which have been analyzed to study the influence of thunderstorm/lightning activity on the ionosphere.

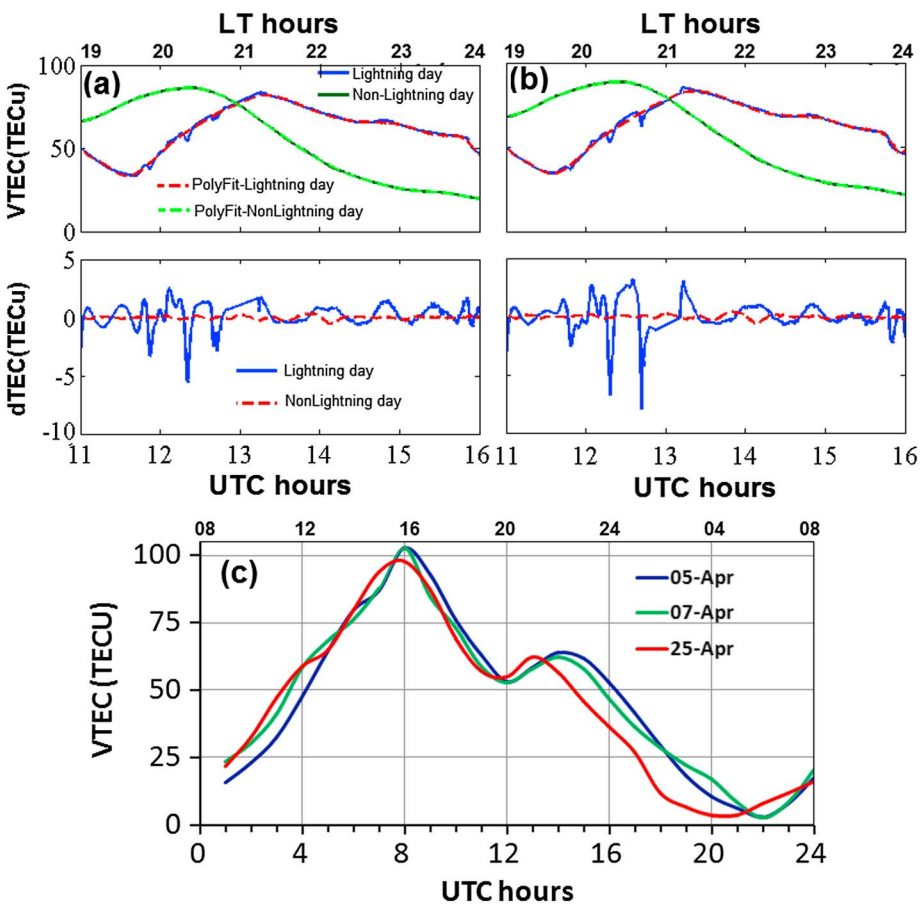


**Figure 3.** VTEC variation along with sixth-order polynomial fit to it against UT hour for PRN 1, deviation in VTEC which is obtained by subtracting undisturbed VTEC from original VTEC for lightning day 1 April 2014 and nonlightning day 7 April 2014 (a) at HKST station, (b) at HKMW station, and (c) diurnal variation of average VTEC estimated from all PRNs during nonlightning days.

Figure 3 shows the VTEC variation along with the best polynomial fit to it and DTEC observed from PRN 1, during 1100–1600 UT, over HKST and HKMW stations. The DTEC curve clearly reveals the enhancement and reduction in TEC values during 1100–1600 UT on the lightning day. On nonlightning day (7 April 2014) during the same time interval TEC shows slight increase around 1100–1230 UT and then decreases with time. In contrast, on the lightning day, TEC decreases with time goes to a minimum (at around 1145 UT) and then increases reaching to a maximum value at around 1315 UT. Further, it decreases slowly with time maintaining higher value than nonlightning day. The lightning day peak value almost coincides with the GPS-TEC value of nonlightning day with a time shift of 45 min. Difference between the minimum and the maximum value of TEC on lightning day is about 48 TECU. During the period (1230–1430) on nonlightning day there is small (30 TECU) decrease in TEC value. An average picture of mean VTEC estimated from all PRNs during three nonlightning geomagnetic quiet days (5, 7, and 25 April 2014) is shown in Figure 3c. Figure 4 shows the variation of VTEC and DTEC for the other two stations HKNP and HKWS for PRN 01 during 1100–1600 UT. At these stations DTEC also shows large perturbations. The difference in TEC value between lightning and nonlightning day at 1300 UT is ~54 TECU and ~53 TECU for the stations HKNP and HKWS, respectively.

Thunderstorms are associated with the generation of electric field and gravity waves, which may reach the ionosphere and perturb ionization distribution which may result in changes in TEC. The upward current associated with thunderstorm causes westward  $E$  field which leads  $E \times B$  plasma drift and plasma moves downward. Lightning-induced pulse interacting with the lower ionosphere may also heat the electron and affect local electron density through ionization, dissociative attachment, and other processes [Inan et al., 1988, 1991; Tarantillo et al., 1993]. In addition to electric field, gravity waves generated during thunderstorm

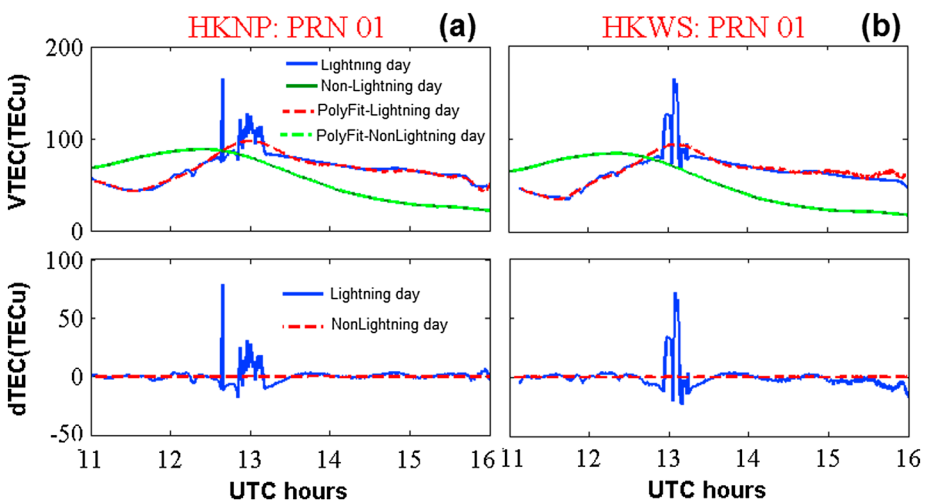


**Figure 4.** VTEC variation along with sixth-order polynomial fit to it against UT hour for PRN 1, deviation in VTEC which is obtained by subtracting undisturbed VTEC from original VTEC for lightning day 1 April 2014 and nonlightning day 7 April 2014 (a) at HKNP station and (b) at HKWS station

activity propagate to the ionosphere and produce electron density enhancement [Lay *et al.*, 2013, 2015]. Gravity waves may take about 1–2 h to reach the lower ionosphere and produce ionization by producing heating effects there [Vadas and Liu, 2009]. Usually, *D* region ionosphere is probed by VLF measurements, whereas GPS-TEC yields information about the whole ionosphere, which has the highest contribution from the *F* region ionosphere.

### 3.2. Gravity Wave Signature in DTEC

Figure 5 shows the normalized DTEC variations computed for PRN 01 over all the GPS stations. Each station is offset vertically from the previous station by 1 TECU. The enhancements as well as depression in DTEC data

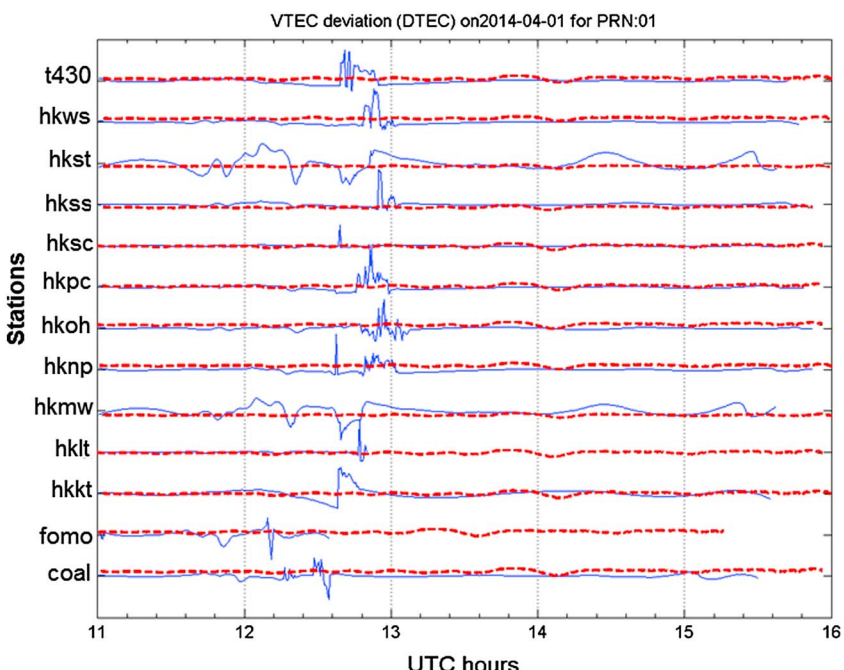


**Figure 5.** Normalized VTEC deviation (DTEC) from best fitted polynomial curve observed with PRN 01 over different GPS stations on 1 April 2014. VTEC deviation on nonlightning day is shown by red dotted curve.

**Table 2.** Period of GWS in DTEC Data Observed From PRN 01 Over Different GPS Stations

Sl. No.	Station Code	Maximum Period (min)
1	COAL	69
2	DSMG	57
3	FOMO	30
4	HKKT	71
5	HKLT	48
6	HKMW	96
7	HKNP	58
8	HKOH	79
9	HKPC	81
10	HKSC	58
11	HKSL	59
12	HKSS	100
13	HKST	80
14	HKWS	62
15	T430	76

in DTEC data suggests that the perturbation is likely to be caused by upward propagating gravity waves generated during lightning/thunderstorm activity. Since the IPP of satellite is moving therefore, it is quite hard to separate periodicity with spatial extent in the case of bubble versus gravity waves. Therefore, we also address the possibility of plasma bubble formation in the following section.

*Yang and Liu* [2016] studied the effect of 2012 tropical Tembin cyclone on the occurrence of ionospheric irregularities using ground- and satellite-based measurements and reported strong scintillation activity in GPS and COSMIC signals over Hong Kong region on the quiet day of 26 August 2012 when cyclone passed close to the Hong Kong. They suggested that the scintillation activity could have been caused by plasma irregularities triggered by the gravity wave generated during cyclone activity in the troposphere that propagated to the ionosphere.

### 3.3. Observation of Plasma Bubbles

Using a method similar to that described by *Portillo et al.* [2008], that defines signatures of plasma bubbles in STEC data, as measured from PRNs 1, 10, 13, 23, and 28, has been noticed during 1100–1900 UT, over several GPS stations in Hong Kong region. For example, Figure 6 shows the plasma bubble signature and ROTI observed during 1100–1900 UT over HKST station from PRNs 1, 10, 23, and 28 on 1 April 2014. At HKST the depth of the bubbles varies from 7 to 55 TECU. The ROTI is found to vary from 3 to 60 TECU/min on the day of lightning (Figure 6), whereas ROTI is insignificant on nonlightning day of 7 April 2014. The plasma bubble signatures observed from PRNs 1, 10, 13, 23, 28, during 1100–1900 UT over the other GPS station HKMW, are shown in Figure 7, and the depth varies from 8 to 65 TECU. ROTI at HKMW is found to vary from 2 to 42 TECU/min. The ROTI variations for PRN 01 over other stations around Hong Kong have also been analyzed, and the peak values are found between 1200 and 1400 UT on the lightning day and almost coincide with the peak current time of lightning discharges. An analysis of plasma bubbles and ROTI during two more nonlightning magnetic quiet days on 3 and 5 April 2014 has also been carried out, but no plasma bubble signatures and significant variation in ROTI have been noticed. *Woodman and Kudeki* [1984] based on observation from Jicamarca Radio Observatory proposed that the increased electric field from thunderstorm activity may lead to plasma instability and plasma bubble in *F* region ionosphere.

The strength of amplitude scintillation in GPS signal is measured by  $S_4$  index which is defined as the ratio of standard deviation of the signal power/intensity to the mean signal power computed over a period of 60 s (1 min). The amplitude scintillation index ( $S_4$ ) is also computed from the GPS station at Hok Sui in Hong Kong for the same PRNs 1, 10, 13, 23, and 28, and the results are shown in Figure 8. The value of  $S_4$  index between 0.25 and 0.5 are usually used for weak scintillations and  $>0.5$  for strong scintillations [*Hlubek et al.*, 2014]. The GPS receiver at Hong Kong Hok Tsui ( $22^{\circ}13'N$ ,  $114^{\circ}15'E$ ) is basically designed for the scintillation studies [*Yang and Liu*, 2016]. From Figure 8 it is noted that the PRNs 1, 10, 13, 23, and 28 show the strong scintillation activity ( $S_4 > 0.5$ ) during 1100–1900 UT. The variation of  $S_4$  index on lightning days is also compared with that on nonlightning day. Scintillation activity on nonlightning day is insignificant ( $S_4 < 0.2$ ) as

have been noted for all the stations lying around the region of lightning activity. The perturbation in TEC has been recorded up to a distance of 500 km and even more between IPPs and the enhanced lightning region. The Morlet wavelet analysis of the DTEC data shows periodicity between 10 min and 100 min. The maximum periodicity observed over each station is listed in Table 2 which shows that the maximum periodicity varies from one station to the other one with the lowest value (30 min) at the FOMO and the largest at the HKSS (~100 min). Observed periodicity

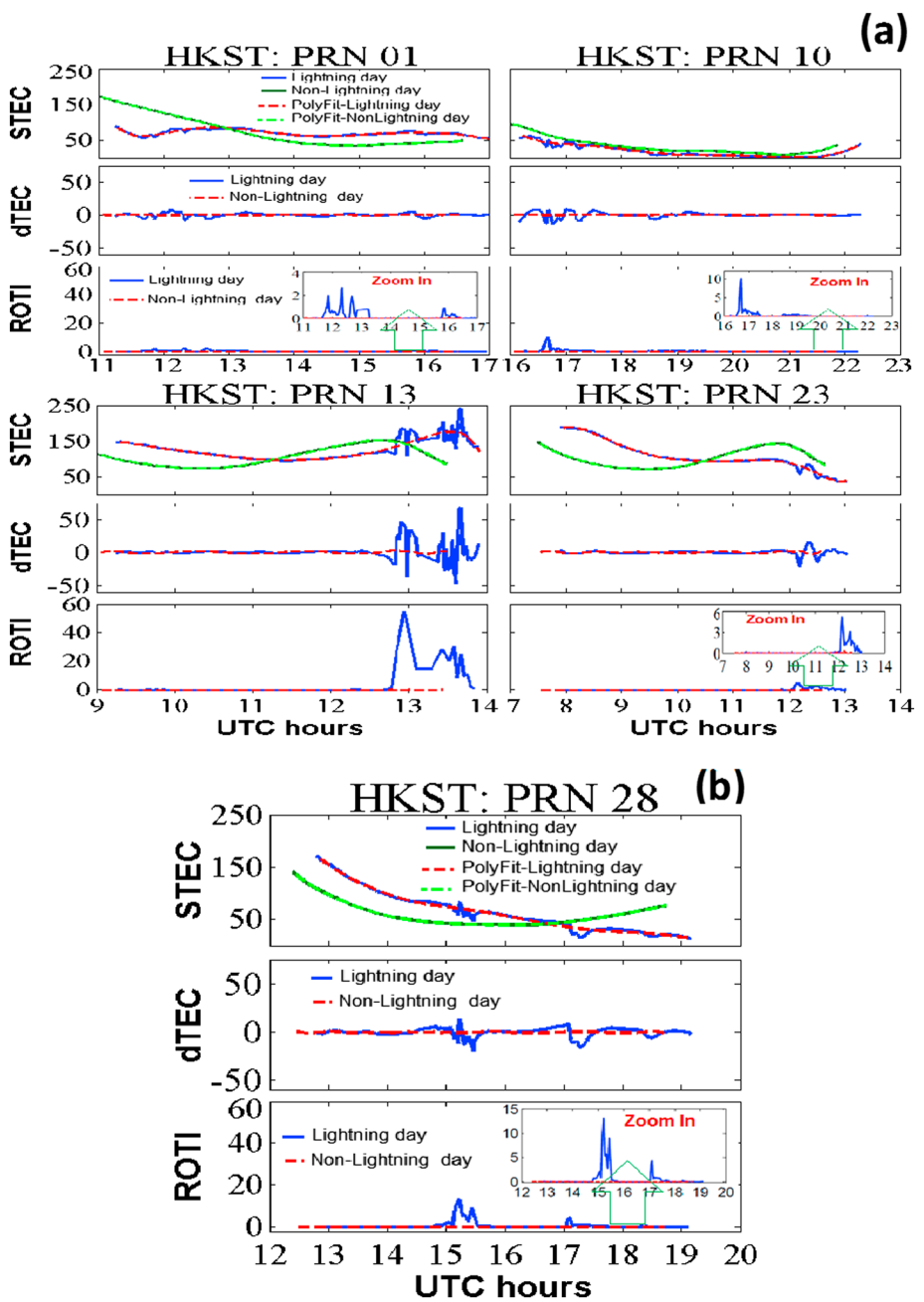


**Figure 6.** (a) Time series of original STEC and best polynomial fitted curve observed by PRNs 1, 10, 13, and 23 at HKST station, in Hong Kong during lightning day of 1 April 2014; the time series of detrended of STEC (dTEC); and the rate of TEC change index (ROTI) expressed in TECU/min showing characteristics of the plasma bubble. Deviation in STEC (DTEC) has been obtained by subtracting the best fitted polynomial curve from the original STEC curve. (b) Same as Figure 6a but for PRN 28.

compared to lightning day. The observed scintillations in respective PRNs at the GPS stations: HKST and HKMW, just confirm that the ionosphere is turbulent.

#### 4. Discussion

The GPS data from Hong Kong CORS network have been used to study the influence of lightning and thunderstorms on ionospheric perturbations. For the lightning activities of 1 April 2014, the ionospheric perturbations in GPS-TEC data have been observed over several GPS stations scattered around the lightning

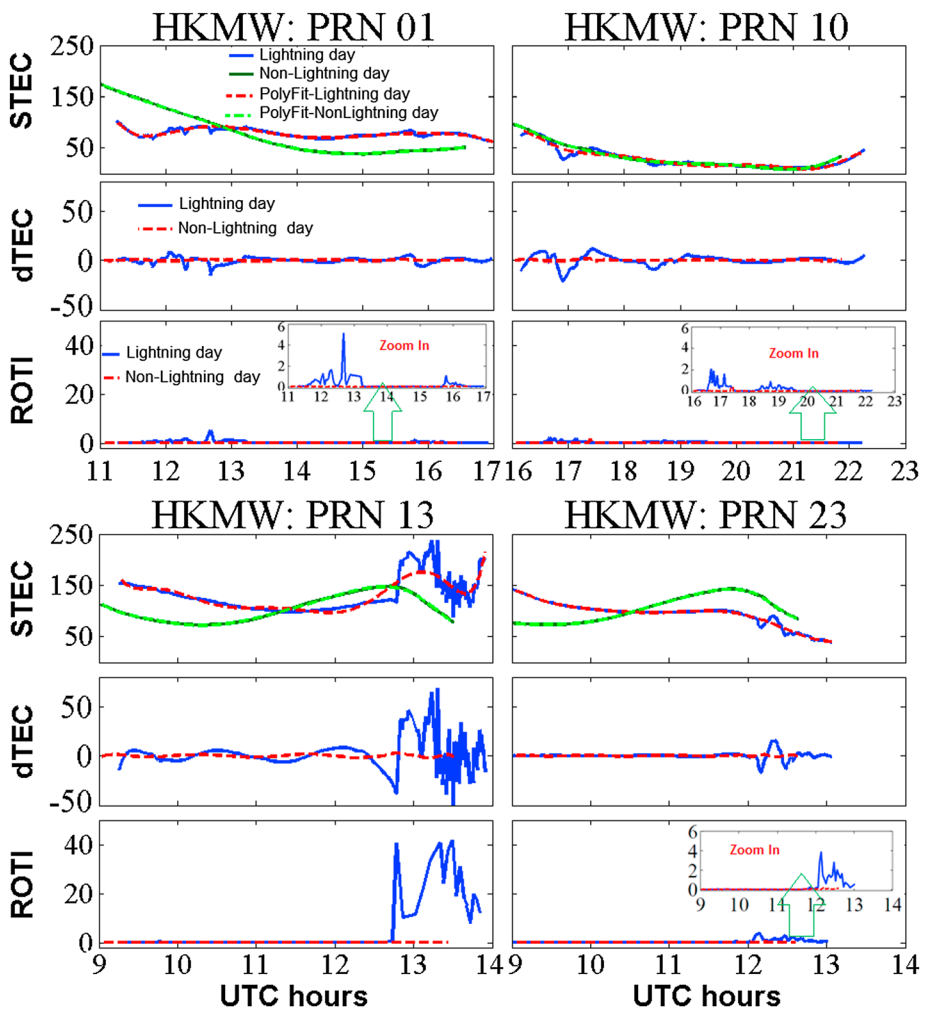


**Figure 7.** Time series of original STEC and best polynomial fitted curve observed by PRNs 1, 10, 13, and 23 at Hkmw station, in Hong Kong during lightning day of 1 April 2014; the time series of detrended of STEC (DTEC) and rate of TEC change index (ROTI) showing characteristics of the plasma bubble. Deviation in STEC (DTEC) has been obtained by subtracting the best fitted polynomial curve from the original STEC curve.

zone and the ROTI values are found to vary up to a maximum of  $\sim 70$  TECU/min. Lay *et al.* [2013] reported lightning-induced perturbation of the ionosphere of  $\sim 1.4$  TECU during nighttime over midlatitude stations (geographic latitude:  $32^{\circ}\text{N}$ – $44^{\circ}\text{N}$ , longitude:  $90^{\circ}\text{W}$ – $104^{\circ}\text{W}$ ) of United States. Vadas and Liu [2009] reported a deviation of  $\sim 2$  TECU ( $\sim 5\%$ ) during a dense convective plume before the sunset and attributed it to the gravity wave generated by the convective plume. It may be noted that the present study shows large change in TEC as compared to earlier studies. This may be due to the fact that present results are from the low-latitude stations where the ionosphere is more sensitive to anomalies/perturbations. Thunderstorm activity/deep convection leads to the generation of gravity waves [Taylor *et al.*, 2009; Sao Sabbas *et al.*, 2009; Vadas *et al.*, 2009; Taylor *et al.*, 2009; Vadas *et al.*, 2009; Chou *et al.*, 2016], which propagating upward could act as seeds in the Mesosphere for the Rayleigh-Taylor instability development [Taylor *et al.*, 2009; Vadas *et al.*, 2009] and generation of plasma bubbles and equatorial spread F in the ionosphere [Vadas and Fritts, 2004]. Interestingly, the wavelet time series analysis of DTEC data associated with lightning activity show periodicity ranging between 10 min to 100 min which may be attributed to thunderstorm induced gravity waves. Vadas and Liu [2013] and Lay *et al.* [2013, 2015] reported thunderstorm associated gravity waves in the region 200–400 km altitude with periods 5 min and longer, whereas there are many reports of the same at lower altitudes (80–100 km) in the D region [Lay and Shao, 2011a, 2011b; Yue *et al.*, 2013; Marshall and Snively, 2014]. Gravity waves may be generated from the overshooting zone of convective thunderstorm plumes [Vadas and Fritts,

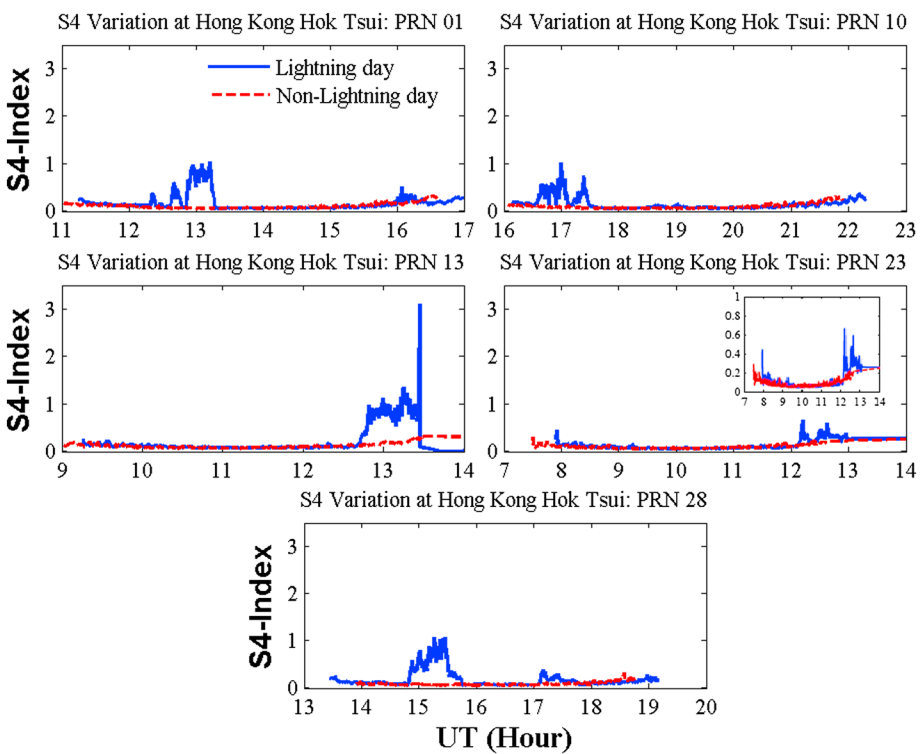


**Figure 8.** Amplitude scintillation index variations against UT hours observed from PRNs 1, 10, 13, 23, and 28 on 1 April 2014 along with nonlightning days of 7 April 2014 over Hong Kong Hok Tsui station.

2004]. Computational results suggest that gravity waves generated from thunderstorm altitude could reach 250–350 km altitude range within 250 km horizontal range from the source [Walterscheid *et al.*, 2003; Zettergren and Snively, 2013].

The upward propagating gravity waves under suitable conditions becomes unstable at higher altitudes and may break (at an altitude around 100 km) into secondary waves [Snively and Pasko, 2003] which continue to propagate upward and can modulate *E* region plasma distribution producing polarization electric fields which maps to *F* region ionosphere [Bishop *et al.*, 2006; Takahashi *et al.*, 2009]. The gravity waves propagating at certain angle with correct amplitude may reach up to the thermosphere and orient to the geomagnetic field in a particular manner and produce ionospheric disturbances [Snively and Pasko, 2003]. Thus, the perturbation in the ionosphere by the thunderstorm activity could be overhead as well as away from the source region by the oblique propagating gravity waves. The observed perturbation in TEC either overhead or away from the thunderstorm zone could be explained.

In addition to triggering of gravity waves, thunderstorms/lightning also perturbs the ionosphere by modifying the electric field and thereby inducing  $E \times B$  drift and Perkins instability [Perkins, 1973]. Based on simulation results, Kuo and Lee [2015] showed the possibility of plasma bubble in the *F* region ionosphere near the thunderstorm location. The eastward electric field caused by charge accumulation on both sides of thunderstorm in association with geomagnetic field lifts low-density plasma upward and triggers the Rayleigh-Taylor instability. Thus, low-density plasma moves upward due to buoyant force in the *F* region high-density plasma as a bubble [Kuo *et al.*, 2014].

In addition to the eastward electric field, the simultaneous presence of a north-south component makes the plasma sheet unstable [Perkins, 1973]. Hamza [1999] showed that the presence of a neutral wind, the gradient in plasma density, and Pedersen conductivity could enhance the growth rate of Perkins instability which plays essential role in the generation of small-scale and kilometer-scale irregularities [Basu *et al.*, 1981]. The reported plasma bubbles (Figures 7 and 8) during the period of intense lightning activity (1100–1800 UT) on 1 April 2014 could be associated with thunderstorms either through Rayleigh-Taylor instability via gravity waves or caused by  $E \times B$  instability via current/electric field modification. Both the processes may contribute

individually or jointly. In the present measurement it is not possible to separate their contributions. In addition to the plasma bubbles, the presence of strong scintillations in the data of PRNs 1, 10, 13, 23, and 28 are also observed (Figure 8) with ROTI variation up to a maximum of 60 TECU/min at a nearby station Hong Kong Hok Tsui which confirms the presence of plasma bubbles and plasma density irregularities. An analysis of data for nonlightning magnetic quiet days (3, 5, and 7 April 2014) did not show the presence of plasma bubble signatures and significant variation in ROTI. However, the plasma bubble occurrences during nonlightning days have been reported in previous works [Nishioka *et al.*, 2008; Kumar *et al.*, 2016]. Generally, equatorial plasma bubbles are formed due to the well-known generalized Rayleigh-Taylor plasma instability mechanism. Recently Kumar *et al.* [2016] studied plasma bubble occurrences and ROTI variations for magnetic quiet days during 2001–2012 over Hong Kong. Their results indicate that most of the plasma bubbles occurred with ROTI less than 2 TECU/min which is much smaller than present results observed on lightning day (up to 60 TECU/min). The present study clearly shows an enhancement of plasma bubbles and/or gravity wave activity over and nearby the lightning-active region. The present study is from the equatorial/low-latitude station where plasma electrodynamics is relatively less studied and more complex. The enhanced depth of the observed plasma bubble could be the result of complex electrodynamic properties of the equatorial ionosphere disturbed by the thunderstorm activity.

## 5. Summary

In the present study perturbation of the ionosphere from disturbances in the troposphere located in the near equatorial region has been investigated. The enhanced ionospheric perturbations in GPS-TEC (DTEC) from the underlying thunderstorm activity observed from several GPS stations over the Hong Kong region, on 1 April 2014 during 1100–1600 UT, for geomagnetic quiet day ( $K_p \leq 4$ ) are reported. Nearly the same method has been used to determine plasma bubbles and gravity waves (GWs). Main conclusions are given below:

The ionospheric perturbation in terms of ROTI is coincident in time and space with lightning activity for this particular case study. The variations in DTEC and ROTI have also been analyzed during nonlightning days of 3, 5, and 7 April 2014 and found to be insignificant in comparison to that with the lightning day.

The ionospheric perturbations in the GPS-TEC (DTEC) show periodic structures with period varying from few minutes to hundreds of minutes. These values are found to lie in the range of 10 min to 100 min, which coincides with the observed thunderstorm-induced gravity waves in the ionosphere [Hocke and Schlegel, 1996; Oliver *et al.*, 1997; Lay *et al.*, 2013]. Further results show that the ionospheric perturbations are observed away from the lightning/thunderstorm source region, which could be attributed to lightning electric field as well as oblique upward propagating gravity waves from tropospheric convective region.

The electric peak current of lightning activity are found to be prominent during local nighttime hour (1100–1800 UT) with a peak at around 1300 UT. During this period a series of plasma bubbles and strong amplitude scintillation activity are detected over many stations of the Hong Kong regions with PRNs 1, 10, 13, 23, and 28. These events are proposed to be associated with thunderstorm-induced electric field which may lead to plasma bubble formation. In addition to electric current, the convectively generated gravity waves during lightning activity and propagating upward to the mesosphere could act as seeds for the growth of the Rayleigh-Taylor instability which also helps in the generation of plasma bubbles [Taylor *et al.*, 2009; Vadas *et al.*, 2009].

From time to time thunderstorm-induced gravity waves as well as associated electric fields have been proposed to explain the observed ionospheric perturbations. It is not possible to find out contribution of individual mechanism. Moreover, ionospheric dynamics is relatively more turbulent and complex at low-latitude region, and hence, more measurements and modeling studies are required to resolve and understand complex atmospheric coupling processes due to lightning/thunderstorm activities.

## References

- Basu, S., S. Basu, S. Ganguly, and J. A. Klobuchar (1981), Generation of kilometer scale irregularities during the midnight collapse at Arecibo, *J. Geophys. Res.*, 86(A9), 7607–7616, doi:10.1029/JA086iA09p07607.  
Bishop, R. L., N. Aponte, G. D. Earle, M. Sulzer, M. F. Larsen, and G. S. Peng (2006), Arecibo observations of ionospheric perturbations associated with the passage of Tropical Storm Odette, *J. Geophys. Res.*, 111, A11320, doi:10.1029/2006JA011668.

## Acknowledgments

The Lands Department of the Government of Hong Kong Special Administrative Region (HKSAR) is acknowledged for providing the GPS data (<http://www.geodetic.gov.hk/smowelcome.htm>). The international GNSS services (IGS) is also acknowledged for GPS data. The work described in this paper was substantially supported by the grant from the European Commission/Research Grants Council (RGC) Collaboration Scheme sponsored by the Research Grants Council of Hong Kong Special Administrative Region, China (project no. E-PolyU 501/16). The support from the RGC project (PolyU 5203/13E, B-Q37X) is acknowledged. Wai Kin Wong at the Hong Kong Observatory is acknowledged for providing the cloud images. SK is thankful to SERB/DST, New Delhi for providing financial support (SR/FTP/ES-164/2014). Authors thank both the reviewers for their valuable comments and suggestions which helped to improve the manuscript quality.

- Burrell, A. G., N. A. Bonito, and C. S. Carrano (2009), Total electron content processing from GPS observations to facilitate ionospheric modeling, *GPS Solut.*, 13(2), 83–95, doi:10.1007/s10291-008-0102-3.
- Chou, C.-C., J. Dai, C.-L. Kuo, and T.-Y. Huang (2016), Simultaneous observations of storm-generated sprite and gravity wave over Bangladesh, *J. Geophys. Res. Space Physics*, 121, 9222–9233, doi:10.1002/2016JA022554.
- Davis, C. J., and C. G. Johnson (2005), Lightning-induced intensification of the ionospheric sporadic E layer, *Nature*, 435(7043), 799–801, doi:10.1038/nature03638.
- Davis, C. J., and K.-H. Lo (2008), An enhancement of the ionospheric sporadic-E layer in response to negative polarity cloud-to-ground lightning, *Geophys. Res. Lett.*, 35, L05815, doi:10.1029/2007GL031909.
- Ding, F., W. Wan, and H. Yuan (2003), The influence of background winds and attenuation on the propagation of atmospheric gravity waves, *J. Atmos. Sol. Terr. Phys.*, 65(7), 857–869, doi:10.1016/S1364-6826(03)00090-7.
- Hamza, A. M. (1999), Perkins instability revisited, *J. Geophys. Res.*, 104(A10), 22,567–22,575, doi:10.1029/1999JA000307.
- Hlubek, N., J. Berdeermann, V. Wilken, S. Gewies, N. Jakowski, M. Wassae, and B. Damtie (2014), Scintillations of the GPS, GLONASS, and Galileo signals at equatorial latitude, *J. Space Weather Space Clim.*, 4, A22, doi:10.1051/swsc/2014020.
- Hocke, K., and K. Schlegel (1996), A review of atmospheric gravity waves and travelling ionospheric disturbances: 1982–1995, *Ann. Geophys.*, 14(9), 917–940, doi:10.1007/s00585-996-0917-6.
- Immel, T. J., S. B. Mende, M. E. Hagan, P. M. Kintner, and S. L. England (2009), Evidence of tropospheric effects on the ionosphere, *Eos Trans. AGU*, 90(9), 69–70, doi:10.1029/2009EO090001.
- Inan, U. S., D. C. Shafer, W. Y. Yip, and R. E. Orville (1988), Subionospheric VLF signatures of nighttime D region perturbations in the vicinity of lightning discharges, *J. Geophys. Res.*, 93(A10), 11,455–11,472, doi:10.1029/JA093iA10p11455.
- Inan, U. S., T. F. Bell, and J. V. Rodriguez (1991), Heating and ionization of the lower ionosphere by lightning, *Geophys. Res. Lett.*, 18(4), 705–708, doi:10.1029/91GL00364.
- Johnson, C. G., and C. J. Davis (2006), The location of lightning affecting the ionospheric sporadic-E layer as evidence for multiple enhancement mechanisms, *Geophys. Res. Lett.*, 33, L07811, doi:10.1029/2005GL025294.
- Kumar, S., and A. K. Singh (2009), Variation of ionospheric total electron content in Indian low latitude region of the equatorial anomaly during May 2007–April 2008, *Adv. Space Res.*, 43(10), 1555–1562, doi:10.1016/j.asr.2009.01.037.
- Kumar, S., E. Tan, and D. Murti (2015), Impacts of solar activity on performance of the IRI-2012 model predictions from low to mid latitudes, *Earth, Planets Space*, 67(1), 42, doi:10.1186/s40623-015-0205-3.
- Kumar, S., W. Chen, Z. Liu, and S. Ji (2016), Effects of solar and geomagnetic activity on the occurrence of equatorial plasma bubbles over Hong Kong, *J. Geophys. Res. Space Physics*, 121, 9164–9178, doi:10.1002/2016JA022873.
- Kumar, V. V., M. L. Parkinson, P. L. Dyson, and G. B. Burns (2009a), The effects of thunderstorm-generated atmospheric gravity waves on mid-latitude F-region drifts, *J. Atmos. Sol. Terr. Phys.*, 71(17), 1904–1915, doi:10.1016/j.jastp.2009.07.006.
- Kumar, V. V., M. L. Parkinson, P. L. Dyson, and G. B. Burns (2009b), Thunderstorm-associated responses in the vertical motion of the mid-latitude F-region ionosphere, *J. Atmos. Sol. Terr. Phys.*, 71, 787–793.
- Kuo, C. L., and L. C. Lee (2015), Ionospheric plasma dynamics and instability caused by upward currents above thunderstorms, *J. Geophys. Res. Space Physics*, 120, 3240–3253, doi:10.1002/2014JA020767.
- Kuo, C. L., L. C. Lee, and J. D. Huba (2014), An improved coupling model for the lithosphere-atmosphere-ionosphere system, *J. Geophys. Res. Space Physics*, 119, 3189–3205, doi:10.1002/2013JA019392.
- Lay, E. H., and X.-M. Shao (2011a), High temporal and spatial-resolution detection of D-layer fluctuations by using time-domain lightning waveforms, *J. Geophys. Res.*, 116, A01317, doi:10.1029/2010JA016018.
- Lay, E. H., and X.-M. Shao (2011b), Multi-station probing of thunderstorm-generated D-layer fluctuations by using time-domain lightning waveforms, *Geophys. Res. Lett.*, 38, L23806, doi:10.1029/2011GL049790.
- Lay, E. H., X. M. Shao, and C. S. Carrano (2013), Variation in total electron content above large thunderstorms, *Geophys. Res. Lett.*, 40, 1945–1949, doi:10.1002/grl.50499.
- Lay, E. H., X. M. Shao, A. K. Kendrick, and C. S. Carrano (2015), Ionospheric acoustic and gravity waves associated with midlatitude thunderstorms, *J. Geophys. Res. Space Physics*, 120, 6010–6020, doi:10.1002/2015JA021334.
- Mareev, E. A., S. A. Yashunin, S. S. Davydenko, T. C. Marshall, M. Stolzenburg, and C. R. Maggio (2008), On the role of transient currents in the global electric circuit, *Geophys. Res. Lett.*, 35, L15810, doi:10.1029/2008GL034554.
- Marshall, R. A., and J. B. Snively (2014), Very low frequency subionospheric remote sensing of thunderstorm-driven acoustic waves in the lower ionosphere, *J. Geophys. Res. Atmos.*, 119, 5037–5045, doi:10.1002/2014JD021594.
- Nishioka, M., A. Saito, and T. Tsugawa (2008), Occurrence characteristics of plasma bubble derived from global ground-based GPS receiver networks, *J. Geophys. Res.*, 113, A05301, doi:10.1029/2007JA012605.
- Oliver, W. L., Y. Otsuka, M. Sato, T. Takami, and S. Fukao (1997), A climatology of F region gravity wave propagation over the middle and upper atmosphere radar, *J. Geophys. Res.*, 102(A7), 14,499–14,512, doi:10.1029/97JA00491.
- Perkins, F. (1973), Spread F and ionospheric currents, *J. Geophys. Res.*, 78(1), 218–226, doi:10.1029/JA078i001p00218.
- Pi, X., A. J. Mannucci, U. J. Lindqwister, and C. M. Ho (1997), Monitoring of global ionospheric irregularities using the Worldwide GPS Network, *Geophys. Res. Lett.*, 24(18), 2283–2286, doi:10.1029/97GL02273.
- Portillo, A., M. Herraiz, S. M. Radicella, and L. Ciralo (2008), Equatorial plasma bubbles studied using African slant total electron content observations, *J. Atmos. Sol. Terr. Phys.*, 70(6), 907–917, doi:10.1016/j.jastp.2007.05.019.
- São Sabbas, F. T., V. T. Rampinelli, J. Santiago, P. Stamus, S. L. Vadas, D. C. Fritts, M. J. Taylor, P. D. Pautet, G. Dolif Neto, and O. Pinto (2009), Characteristics of sprite and gravity wave convective sources present in satellite IR images during the SpreadFEx 2005 in Brazil, *Ann. Geophys.*, 27, 1279–1293.
- Shao, X.-M., E. H. Lay, and A. R. Jacobson (2012), Reduction of electron density in the night-time lower ionosphere in response to a thunderstorm, *Nat. Geosci.*, 6(1), 29–33, doi:10.1038/ngeo1668.
- Singh, D., R. P. Singh, A. K. Singh, S. Kumar, M. N. Kulkarni, and A. K. Singh (2012), Discharges in the stratosphere and mesosphere, *Space Sci. Rev.*, 169(1–4), 73–121, doi:10.1007/s11214-012-9906-0.
- Snively, J. B., and V. P. Pasko (2003), Breaking of thunderstorm-generated gravity waves as a source of short-period ducted waves at mesopause altitudes, *Geophys. Res. Lett.*, 30(24), 2254, doi:10.1029/2003GL018436.
- Takahashi, H., et al. (2009), Simultaneous observation of ionospheric plasma bubbles and mesospheric gravity waves during the SpreadFEx Campaign, *Ann. Geophys.*, 27(4), 1477–1487, doi:10.5194/angeo-27-1477-2009.
- Taranenko, Y. N., U. S. Inan, and T. F. Bell (1993), The interaction with the lower ionosphere of electromagnetic pulses from lightning: Heating, attachment, and ionization, *Geophys. Res. Lett.*, 20(15), 1539–1542, doi:10.1029/93GL01696.

- Taylor, M. J., P.-D. Pautet, A. F. Medeiros, R. Buriti, J. Fechine, D. C. Fritts, S. L. Vadas, H. Takahashi, and F. T. São Sabbas (2009), Characteristics of mesospheric gravity waves near the magnetic equator, Brazil, during the SpreadFEx campaign, *Ann. Geophys.*, 27(2), 461–472, doi:10.5194/angeo-27-461-2009.
- Vadas, S. L., and D. C. Fritts (2004), Thermospheric responses to gravity waves arising from mesoscale convective complexes, *J. Atmos. Sol. Terr. Phys.*, 66(6), 781–804, doi:10.1016/j.jastp.2004.01.025.
- Vadas, S. L., and H. L. Liu (2009), Generation of large-scale gravity waves and neutral winds in the thermosphere from the dissipation of convectively generated gravity waves, *J. Geophys. Res.*, 114, A10310, doi:10.1029/2009JA014108.
- Vadas, S. L., and H.-L. Liu (2013), Numerical modeling of the large-scale neutral and plasma responses to the body forces created by the dissipation of gravity waves from 6 h of deep convection in Brazil, *J. Geophys. Res. Space Physics*, 118, 2593–2617, doi:10.1002/jgrs.50249.
- Vadas, S. L., M. J. Taylor, P.-D. Pautet, P. A. Stamus, D. C. Fritts, H.-L. Liu, F. T. São Sabbas, V. T. Rampinelli, P. Batista, and H. Takahashi (2009), Convection: The likely source of the medium-scale gravity waves observed in the OH airglow layer near Brasilia, Brazil, during the SpreadFEx campaign, *Ann. Geophys.*, 27(1), 231–259, doi:10.5194/angeo-27-231-2009.
- Vellinov, P., C. Spassov, and S. Kolev (1992), Ionospheric effects of lightning during the increasing part of solar cycle 22, *J. Atmos. Terr. Phys.*, 54(10), 1347–1353, doi:10.1016/0021-9169(92)90044-L.
- Walterscheid, R. L., G. Schubert, and D. G. Brinkman (2003), Acoustic waves in the upper mesosphere and lower thermosphere generated by deep tropical convection, *J. Geophys. Res.*, 108(A11), 1392, doi:10.1029/2003JA010065.
- Williams, E. R. (2009), The global electrical circuit: A review, *Atmos. Res.*, 91(2–4), 140–152, doi:10.1016/j.atmosres.2008.05.018.
- Woodman, R. F., and E. Kudeki (1984), A causal relationship between lightning and explosive spread F, *Geophys. Res. Lett.*, 11(12), 1165–1167, doi:10.1029/GL011i012p01165.
- Yang, Z., and Z. Liu (2016), Observational study of ionospheric irregularities and GPS scintillations associated with the 2012 tropical cyclone Tembin passing Hong Kong, *J. Geophys. Res. Space Physics*, 121, 1–13, doi:10.1002/2016JA022398.Received.
- Yue, J., S. L. Vadas, C.-Y. She, T. Nakamura, S. C. Reising, H.-L. Liu, P. Stamus, D. A. Krueger, W. Lyons, and T. Li (2009), Concentric gravity waves in the mesosphere generated by deep convective plumes in the lower atmosphere near Fort Collins, Colorado, *J. Geophys. Res.*, 114, D06104, doi:10.1029/2008JD011244.
- Yue, J., L. Hoffmann, and M. Joan Alexander (2013), Simultaneous observations of convective gravity waves from a ground-based airglow imager and the AIRS satellite experiment, *J. Geophys. Res. Atmos.*, 118, 3178–3191, doi:10.1002/jgrd.50341.
- Zettergren, M. D., and J. B. Snively (2013), Ionospheric signatures of acoustic waves generated by transient tropospheric forcing, *Geophys. Res. Lett.*, 40, 5345–5349, doi:10.1002/2013GL058018.

## Erratum

In the originally published version of this article, Figure 1 incorrectly displayed two identical color bars. The figure has been corrected, and the present version may be considered the authoritative version of record.